Plant Soil (2019) 442:233–246
https://doi.org/10.1007/s11104-019-04179-7

REGULAR ARTICLE

Exotic *Spartina alterniflora* invasion alters soil nitrous oxide emission dynamics in a coastal wetland of China

Dengzhou Gao · Lijun Hou · Xiaofei Li · Min Liu · Yanling Zheng · Guoyu Yin · Yi Yang · Cheng Liu · Ping Han

Received: 28 December 2018 / Accepted: 18 June 2019 / Published online: 4 July 2019

Abstract

Aims Exotic *Spartina alterniflora* invasion resulting from anthropogenic activities significantly affects microbial nitrogen (N) transformation and associated nitrous oxide (N_2O) emission in coastal wetland soils. However, the responses of soil N_2O emission dynamics to plant invasion remain unclear. This study assesses the effects of *S. alterniflora* invasion on soil N_2O potential production and consumption processes.

Methods We used natural isotope tracing technique to investigate potential N_2O production and consumption rates in *S. alterniflora* invaded and native saltmarsh zones (*Phragmites australis*, *Scirpus mariqueter* and bare mudflat) in the Yangtze Estuary.

Results Soil potential net N_2O production rates in summer were lower in *S. alterniflora* stands than in *S. mariqueter* and bare mudflat stands, but no significant differences among these saltmarsh habitats occurred during winter. Potential gross N_2O production and consumption rates were higher in *S. alterniflora* and *P. australis* stands compared to *S. mariqueter* and bare mudflat stands. The gross consumption proportion in *S. alterniflora* and *P. australis* stands was higher, which affected net N_2O production. Hydroxylamine (NH_2OH) oxidation and nitrifier denitrification contributed 4.52–12.62% and 13.87–21.58% of soil N_2O source, respectively, but denitrification was the dominant pathway (69.83–80.09%). *S. alterniflora* invasion increased the contributions of NH_2OH oxidation and nitrifier denitrification to N_2O source slightly, but decreased the contribution of denitrification to N_2O source. Soil potential N_2O production and consumption processes were influenced by water-filled pore space, pH, sulfide, and carbon and N substrates.

Conclusion Exotic *S. alterniflora* invasion affected soil N_2O dynamics by increasing substrates and altering microenvironments, thus mediating N_2O emission from coastal saltmarsh soils.

Keywords Nitrous oxide · Dynamics · Saltmarsh wetland · *Spartina alterniflora* · Yangtze estuary

Dengzhou Gao and Lijun Hou contributed equally to this work.

Responsible Editor: Sven Marhan.

Electronic supplementary material The online version of this article (https://doi.org/10.1007/s11104-019-04179-7) contains supplementary material, which is available to authorized users.

D. Gao · M. Liu (✉) · Y. Zheng · G. Yin · Y. Yang · P. Han
College of Geographical Sciences, East China Normal University, 500 Dongchuan Road, Shanghai 200241, China
e-mail: mliu@geo.ecnu.edu.cn

D. Gao · L. Hou (✉) · Y. Zheng · Y. Yang · C. Liu · P. Han
State Key Laboratory of Estuarine and Coastal Research, East China Normal University, 3663 North Zhongshan Road, Shanghai 200062, China
e-mail: ljhou@sklec.ecnu.edu.cn

X. Li
Key Laboratory for Humid Subtropical Eco-geographical Processes of the Ministry of Education, Fujian Normal University, 8 Shangsan Road, Fuzhou 350007, China

Introduction

Nitrogen (N) loading from industrial and agricultural activities affects estuarine wetland ecosystems (Canfield et al. 2010). Estuarine and coastal soils are hotspots of N biogeochemical cycling (Bowden 1986; Onley et al. 2018). Microbial N transformation may be accompanied by production of nitrous oxide (N_2O), a potent greenhouse gas and potential destroyer of ozone layer (Ravishankara et al. 2009). Estuarine saltmarshes are significant sources of N_2O, which account for about 60% of global marine N_2O emission (Dong et al. 2002). Continuous atmospheric N_2O concentration increase suggests the need to measure N_2O emission in these aquatic ecosystems (Butterbach-Bahl et al. 2013).

N_2O emission from natural environments are complicated, because N_2O is produced by various microbial N transformation processes, and is consumed/ decomposed simultaneously (Robertson 1987; Firestone and Davidson 1989; Toyoda et al. 2011). Microbial N_2O production pathways generally include hydroxylamine (NH_2OH) oxidation, denitrification, nitrifier denitrification and fungal denitrification (Shoun and Tanimoto 1991; Wrage et al. 2001; Toyoda et al. 2011). Denitrification is an important N_2O consumption pathway, and recognized as a primary process controlling N_2O emission (Cohen and Gordon 1978; Firestone and Davidson 1989; Toyoda et al. 2011). Estuarine saltmarsh wetlands are sensitive to environmental changes, and plant communities affect soil microbial N biogeochemical processes (Stribling and Cornwell 2001; Sun et al. 2015). The exotic *Spartina alterniflora*, a perennial C_4 plant, was introduced to China in 1979 to stabilize soil and protect the coastline (Li et al. 2009) and has expanded over the past 30 years. As a dominant plant in the coastal area of China, it now threatens the sustainability of coastal ecosystems (Lu and Zhang 2013). Compared to most native plants, exotic *S. alterniflora* has higher plant biomass, root system and net primary productivity, which alters soil physico-chemical properties (Zhang et al. 2013; Yang et al. 2016) and affects N cycling. Until now, extensive studies have reported that *S. alterniflora* invasion significantly impacts soil key N transformation processes (Peng et al. 2011; Zheng et al. 2016; Gao et al. 2017). There are also many studies concerning about soil N_2O emission affected by *S. alterniflora* invasion, but the extent remains uncertain (Yuan et al. 2015). For instance, *S. alterniflora* enhances soil carbon and N pool due to increased biomass inputs, and may stimulate N_2O production (Cheng et al. 2007; Zhang et al. 2013). Conversely, *S. alterniflora* may suppress N_2O production because of increased uptake of N (Yuan et al. 2015; Jia et al. 2016). Revealing soil N_2O production and consumption processes helps explain the effects of *S. alterniflora* invasion on N_2O emission (Yang and Silver 2016).

The N_2O production and consumption rates are associated with availability of N and total organic carbon (TOC) substrates (Allen et al. 2007; Wunderlin et al. 2013; Zhang et al. 2013). The transformations are also affected by environmental factors such as temperature, moisture, texture, oxidative-reductive conditions and pH (Sørensen et al. 1980; Butterbach-Bahl et al. 2013; Yang and Silver 2016). Furthermore, the N transformation processes may interact with each other; for example, dissimilatory nitrate reduction to ammonium (DNRA) compete with denitrification for electron donors, which may indirectly alter soil N_2O production processes (Tiedje et al. 1983; Yang and Silver 2016). However, the processes and factors dominating the responses of N_2O dynamics to *S. alterniflora* invasion are not well understood. An improved understanding of the influences of *S. alterniflora* invasion on soil N_2O production/consumption processes and their controlling factors is essential to advance effective strategies for N_2O mitigation and management of plant invasion in these ecosystems.

Previous studies used $^{15}N_2O$ pool dilution techniques to determine gross N_2O production and consumption simultaneously, but this approach does not distinguish N_2O production from specific processes (Yang et al. 2011). With the evolution of isotopic techniques, nitrogen and oxygen stable isotope ratios of N_2O are applied to elucidate N_2O dynamics in natural ecosystems (Toyoda et al. 2011; Zou et al. 2014; Wei et al. 2017; Murray et al. 2018). Nitrous oxide is an asymmetric linear N-N-O molecule, and the abundance of $^{14}N^{15}N^{16}O$ and $^{15}N^{14}N^{16}O$ relative to $^{14}N^{14}N^{16}O$ can provide detailed information on N_2O formation and decomposition processes (Sutka et al. 2003). The ^{15}N site preference (SP, the difference in $^{15}N/^{14}N$ ratio between central (α site) and terminal (β site) N atoms in the $^{\beta}N\text{-}^{\alpha}N\text{-}O$ molecule) value of N_2O can identify its source and the proportion of N_2O reduction to N_2 (Koba et al. 2009; Toyoda et al. 2011; Zou et al. 2014). However, detailed N_2O natural-abundance isotopic analysis is limited in estuarine saltmarsh wetlands.

Estuarine saltmarsh wetlands are subject to tidal action, N overloading and exotic plant invasion which complicate N_2O dynamics (Sun et al. 2015). Nevertheless, their sensibility to environmental changes has attracted limited attention compared to terrestrial and

marine ecosystems (Murray et al. 2018). Therefore, we conducted an experiment to reveal the effects of *S. alterniflora* invasion on soil N_2O emission in the Yangtze estuarine wetland of China. The objectives of this study are: (i) to investigate soil potential N transformation processes, net N_2O production rates and its isotopic signatures ($\delta^{15}N$, $\delta^{18}O$ and SP of N_2O), (ii) to determine whether exotic *S. alterniflora* invasion alters soil gross N_2O production and consumption processes based on natural isotopic signatures, and (iii) to identify key environmental factors affecting N_2O dynamics in the *S. alterniflora* invasion wetlands. This study improves understanding of the mechanisms driving N_2O emission in estuarine saltmarsh wetlands undergoing exotic plant invasion.

Materials and methods

Study areas and sample collection

The study area is located in the Dongtan saltmarsh wetland of the Yangtze estuary (30°25′-31°38′N, 121°50′-122°05′E, Fig. S1). This region is characterized by a typically semi-tropical monsoon climate (Wang et al. 2007). The soil in this area is dominated by clay and silt, with mean grain sizes of 23.1–102.5 μm (Yin et al. 2017). This area is overgrown with saltmarsh plants, and *Phragmites australis* and *Scirpus mariqueter* are the dominant native plants. *S. alterniflora* was introduced to China in 1979, and has rapidly expanded to compete with native plant communities in the coastal saltmarsh wetlands of China, including the Yangtze estuary (Li et al. 2009). In this study, we selected an approximately 1200 m long transect spanning the bare mudflat, *S. mariqueter*, *S. alterniflora* (invading for approximately 10 years) and *P. australis* communities. In each plant community stand, three soil samples (0–5 cm) were collected randomly using 15-cm diameter stainless steel soil cylinders in July 2017 and January 2018. The distance between replicates was approximately 40–50 m. A cutting ring (5 cm in diameter and 5 cm in height) was pressed into collected undisturbed soil for the determination of bulk density and water content (Lu 2000). After collection, soil samples were placed into sterile plastic bags and stored at 4 °C cooler. All samples were transported to the laboratory within 3 h for subsequent analyses of soil characteristics, potential N transformation and N_2O dynamics.

Analysis of soil properties and potential N transformation processes

Soil gravimetric water content and dry bulk density were measured by the oven drying method and the cutting-ring method, respectively (Lu 2000). Soil water filled pore space (WFPS) was calculated using the method described by Allen et al. (2007). Soil pH and salinity were determined with a Mettler-Toledo pH meter and YSI-30 portable salinity meter, after soil was mixed with CO_2-free deionized water at a 1:2.5 ratio (w:v) (Yin et al. 2017). Soil TOC was determined using a CHNS analyzer (Vario EL, Elementar, Germany) after acidification with 1 M HCl (Gao et al. 2017) to remove carbonate. Soil NH_4^+, NO_3^-, and NO_2^- were extracted with 2 M KCl, and their concentrations determined via flow injection analysis (Skalar Analytical SAN++, Netherlands) (Zhang et al. 2015). The isotopic compositions of soil NH_4^+ and NO_3^-, including $\delta^{15}N\text{-}NH_4^+$, $\delta^{15}N\text{-}NO_3^-$ and $\delta^{18}O\text{-}NO_3^-$, were determined using the diffusion and denitrifier methods in combination with MAT 253 Plus IRMS facility (ThermoFinnigan, Bremen, Germany), respectively (Wu et al. 2018). Total extractable Fe, ferrous oxides (Fe(II)) and ferric iron (Fe(III)) of soil were determined using the ferrozine method (Lovley and Phillips 1987). Soil sulfide concentrations were spectrophotometrically determined using methylene blue (Cline 1969). Grain sizes of soil were analyzed via Mastersizer 2000 laser diffraction (Malvern Instruments Ltd., UK).

Potential nitrification rates of soil were determined using a modified chlorate inhibition method (Dollhopf et al. 2005). In brief, 10 g of fresh soil (equivalent to approximately 6.06 g dry soil) was placed into Erlenmeyer flasks, containing 50 mL of filter-sterilized in situ tidal water amended with 0.5 mM $(NH_4)_2SO_4$ and 10 mM $KClO_3$. Triplicate slurries of each sample were incubated in the dark at near in situ temperature (32 °C for summer and 5 °C for winter). All flasks were shaken (150 rpm) on a reciprocating shaker for 12 h, and 5 mL of subsample was withdrawn at 3 h intervals for analysis of NO_2^-. The $KClO_3$ blocked nitrite oxidation, so potential nitrification rates were estimated from linear regressions of NO_2^- production over time (Dollhopf et al. 2005).

Potential rates of denitrification and anaerobic ammonium oxidation (ANAMMOX) and DNRA were measured by soil slurry experiments using nitrogen isotope-tracing techniques (Thamdrup and Dalsgaard 2002; Deng et al. 2015). Specifically, soil slurries were

made with fresh soil and tidal water at a 1:7 ratio. After purging with helium for about 30 min, samples were transferred into helium-purged 12 mL vials (Exetainer, Labco). All vials were pre-incubated for 36 h to remove background NO_3^-/NO_2^- at near-field temperature (32 °C for summer and 5 °C for winter). After pre-incubation, the vials were spiked with 100 μL sterile anoxic solutions of $^{15}NO_3^-$ (12.5 mM, ^{15}N at 99%) through septa (final concentration of $^{15}NO_3^-$ in each vial was approximately 100 μM). Saturated $ZnCl_2$ (200 μL) was added to one half of the vials (initial samples) to stop any further chemical reactions. The remaining final sample vials were incubated for 8 h, and stopped by injecting 200 μL saturated $ZnCl_2$ at the end of incubation. Concentrations of $^{29}N_2$ and $^{30}N_2$ in incubation vials were determined by membrane inlet mass spectrometry, and potential rates of denitrification and ANAMMOX were calculated by the $^{29}N_2$ and $^{30}N_2$ produced between final and initial samples as described by Deng et al. (2015). The occurrence of ANAMMOX at all stands was confirmed by a preliminary tracer experiment of $^{15}NH_4^+$ (Hou et al. 2013). Meanwhile, the concentrations of $^{15}NH_4^+$ produced in the $^{15}NO_3^-$ treatment were determined using ammonium oxidation membrane inlet mass spectrometry (OX/MIMS) to estimate the potential DNRA rates (Yin et al. 2014). More detailed information on the slurry incubation experiments is given in Supplementary Material.

Determination of soil potential net N_2O production and isotopic signatures

Fresh soils (100 g, equivalent to approximately 60.6 g dry soil) were placed into 500-mL incubation bottles equipped with three-way stopcocks (Fig. S2), and then flushed with high-purity air (O_2: N_2 = 21: 79) through three-way stopcocks for 20 min to eliminate background N_2O. Immediately, after flushing, the bottles were sealed and incubated in the dark at near-field temperature (32 °C for summer and 5 °C for winter) for 8 h. Gas samples were collected via polypropylene syringes at the beginning and end of the incubations, respectively. The N_2O concentrations in gas samples were determined by gas chromatography (GC-2014, Shimadzu, Kyoto, Japan), and potential net N_2O production rates were calculated as follows (Zhang et al. 2016):

$$F_{\text{Net production}} = \frac{dc}{dt} \times \frac{V_H}{M_S} \times \frac{M_W}{M_V} \times \frac{T_{st}}{T_{st} + T} \quad (1)$$

where $F_{\text{Net production}}$ is soil potential N_2O net production rates (nmol g^{-1} h^{-1}); $\frac{dc}{dt}$ represents N_2O concentration increase (μL L^{-1} h^{-1}); V_H and M_S are the volume of headspace (L) and the weight of soil (g), respectively; M_W is the molecular weight (g mol^{-1}), and M_V is the volume of one mole of ideal gas (L mol^{-1}); T is the incubation temperature (°C), and T_{st} is standard temperature (K).

N_2O isotopic signatures, including $\delta^{15}N$, $\delta^{15}N^{\alpha}$ and $\delta^{18}O$, were measured using isotope ratio mass spectrometry (IRMS, Isoprime100, Isoprime, Cheadle, UK) (Zhang et al. 2016). The isotope values are reported using delta notation as per mil versus atmospheric N_2 for N and Vienna Standard Mean Ocean Water (VSMOW) for O ($\delta X = (R_{\text{sample}}/R_{\text{std}} - 1) \times 1000‰$, X = ^{15}N, $^{15}N^{\alpha}$ and ^{18}O). The $\delta^{15}N^{\beta}$ value was calculated by $\delta^{15}N^{\beta} = 2 \times \delta^{15}N^{\text{bulk}} - \delta^{15}N^{\alpha}$, and $SP = \delta^{15}N^{\alpha} - \delta^{15}N^{\beta}$ (Toyoda et al. 2011). The analytical precisions of $\delta^{15}N^{\text{bulk}}$, $\delta^{15}N^{\alpha}$ and $\delta^{18}O$ were 0.5‰, 0.9‰ and 0.6‰, respectively.

Measurement of potential gross N_2O production and consumption

Potential gross N_2O production rates were calculated from potential net N_2O production and gross N_2O consumption proportion, which are expressed as follows:

$$F_{\text{Gross production}} = \frac{F_{\text{Net production}}}{100 - P_{\text{Gross consumption}}} \quad (2)$$

where $F_{Gross\ production}$ and $F_{Net\ production}$ are the potential rates of gross N_2O production and net N_2O production rates (nmol g^{-1} h^{-1}), respectively; $P_{Gross\ consumption}$ denotes the proportion of gross N_2O consumption (%), which can be calculated based on the modified equation (Toyoda et al. 2011):

$$P_{\text{Gross consumption}}(\%) = \left(1 - e^{\frac{-SP_{\text{sediment}} + SP^*_{\text{sediment}}}{\varepsilon(SP)red}}\right) \times 100\% \quad (3)$$

where SP_{sediment} and SP^*_{sediment} denote the measured SP-N_2O values and initial SP-N_2O values corrected for reduction effect, respectively; $\varepsilon(SP)red$ denotes the enrichment factor (−5.9‰) for SP of N_2O reduction (Ostrom et al. 2007). Here, $SP^*_{sediment}$ was estimated by the Monte Carlo method based on the average reduction slope (1.12 ± 0.12, the ratio of fractionation factors for

SP and $\delta^{15}N$ during N_2O reduction; Fig. S3), as described by Toyoda et al. (2011) and Ishii et al. (2014). By combining the potential rates of gross N_2O production and net N_2O production, we obtained potential gross N_2O consumption rates ($F_{\text{Gross consumption}}$) (nmol g^{-1} h^{-1}) as presented below:

$$F_{\text{Gross consumption}} = F_{\text{Gross production}} - F_{\text{Net production}} \quad (4)$$

In addition, the source of N_2O can be quantified from $SP^*_{sediment}$ values based on a two-endmember mixing model (Toyoda et al. 2011; Deppe et al. 2017). Cycloheximide inhibition experiments (inhibiting fungal activity) indicated that N_2O production via fungal denitrification was small (Table S1), so the contribution of fungal denitrification to N_2O source was not considered in this study. The detailed information on cycloheximide inhibition experiment is given in Supplementary Material. In this case, we were concerned mainly about the pathways of NH_2OH oxidation and bacteria denitrification (including denitrification and nitrifier denitrification) (Ishii et al. 2014). The SP-N_2O values are approximately 35‰ for NH_2OH oxidation and − 5‰ for bacteria denitrification (Toyoda et al. 2005; Sutka et al. 2006), and the relative contributions of NH_2OH oxidation and bacteria denitrification to N_2O emission can be estimated as follows (Deppe et al. 2017):

$$C_{\text{NH}_2\text{OH oxidation}}(\%) = \frac{SP^*_{\text{sample}} - SP_{\text{bacteria denitrification 1}}}{SP_{\text{NH}_2\text{OH oxidation}} - SP_{\text{bacteria denitrification}}} \times 100\% \quad (5)$$

$$C_{\text{bacteria denitrification}}(\%) = 100 - C_{\text{NH}_2\text{OH oxidation}} \quad (6)$$

where $C_{\text{NH}_2\text{OH oxidation}}$ and $C_{\text{bacteria denitrification}}$ denote the contributions of soil N_2O derived from NH_2OH oxidation and bacteria denitrification processes, respectively; $SP_{\text{NH}_2\text{OH oxidation}}$ and $SP_{\text{bacteria denitrification}}$ represent the average *SP*-N_2O values produced by NH_2OH oxidation (35‰) and bacteria denitrification (−5‰) processes, respectively (Toyoda et al. 2005; Sutka et al. 2006).

C_2H_2 inhibition experiments were conducted to quantify the contributions of denitrification to soil N_2O source (Zhu et al. 2013), which further distinguished the contributions of denitrification and nitrifier denitrification in combination with isotopic analysis (Deppe et al. 2017). In brief, 100 g of fresh soil (equivalent to approximately 60.6 g dry soil) was placed into the incubation bottles and purged with pure air for 20 min, and these bottles were injected with 0.01% (vol/vol) C_2H_2 gas. Specific incubation and measurement programs are the same as described above. The contributions of denitrification and nitrifier denitrification to soil N_2O source are calculated as follows:

$$C_{\text{denitrification}}(\%) = \frac{F_{+C_2H_2\text{ production}}}{F_{\text{Net production}}} \times 100\% \quad (7)$$

$$C_{\text{nitrifier denitrification}}(\%) = C_{\text{bacteria denitrification}} - C_{\text{denitrification}} \quad (8)$$

where $C_{\text{denitrification}}$ and $C_{\text{nitrifier denitrification}}$ are the contributions of denitrification and nitrifier denitrification to N_2O source, respectively; $F_{+C_2H_2\text{ production}}$ is N_2O production in the C_2H_2 treatments, and $F_{\text{Net production}}$ is the net N_2O production.

Statistical analysis

All data sets were checked to satisfy the assumptions of homogeneity and normality. One-way ANOVA was used to determine differences in soil parameters. Multiple stepwise regression was used to measure soil variables that could explain the variations of net N_2O production rates and pathways effectively. Level of significance was chosen at $p < 0.05$. All statistical analyses were conducted using SPSS 19.0 software (SPSS, Inc., Chicago, IL, USA).

Results

Soil characteristics and potential N transformation rates

Soil WFPS in *S. alterniflora* stands (45.16 ± 5.85% for summer; 48.11 ± 5.63% for winter) was generally lower than that of *S. mariqueter* stand and bare mudflat. The bulk density also was lower in *S. alterniflora* (0.77 ± 0.08 g cm^{-3} for summer; 0.73 ± 0.05 g cm^{-3} for winter) than in other stands (Table 1). Soil pH and salinity ranged from 7.82 to 8.32 and 0.64 to 1.24, respectively, with no significant difference among the saltmarsh zones (Table 1). Soil TOC and sulfide concentrations in *S. alterniflora* stands were significantly higher than those in bare mudflat and *S. mariqueter* stands, but comparable to those in *P. australis* stands (Table 1). Soil NH_4^+ and NO_2^- were generally higher in *S. alterniflora*

Table 1 Soil physico-chemical characteristics across the saltmarsh stands

	Summer				Winter			
	Bare mudflat	*S. mariqueter*	*P. australis*	*S. alterniflora*	Bare flat	*S. mariqueter*	*P. australis*	*S. alterniflora*
WFPS (%)†	64.11 ± 6.10 ^{a}	64.15 ± 2.16 ^{a}	46.25 ± 3.71 ^{b}	45.16 ± 5.85 ^{b}	52.94 ± 2.51 ^{a}	52.26 ± 6.85 ^{ab}	45.81 ± 2.78 ^{b}	48.11 ± 5.63 ^{ab}
Bulk density (g cm^{-3}) †	1.05 ± 0.09 ^{a}	1.07 ± 0.08 ^{a}	1.01 ± 0.09 ^{a}	0.77 ± 0.08 ^{b}	0.79 ± 0.02 ^{a}	0.82 ± 0.07 ^{a}	0.73 ± 0.02 ^{a}	0.73 ± 0.05 ^{a}
pH	8.32 ± 0.28 ^{a}	8.31 ± 0.21 ^{a}	8.15 ± 0.22 ^{a}	7.90 ± 0.02 ^{a}	8.29 ± 0.04 ^{a}	8.11 ± 0.21 ^{ab}	8.17 ± 0.06 ^{ab}	7.82 ± 0.16 ^{b}
Salinity	0.71 ± 0.09 ^{a}	0.64 ± 0.08 ^{a}	0.80 ± 0.09 ^{a}	0.70 ± 0.03 ^{a}	1.24 ± 0.28 ^{a}	0.94 ± 0.11 ^{a}	0.88 ± 0.06 ^{a}	0.86 ± 0.15 ^{a}
TOC (g kg^{-1}) †, §	19.44 ± 1.51 ^{b}	21.13 ± 1.47 ^{b}	26.27 ± 2.02 ^{a}	27.66 ± 1.81 ^{a}	14.35 ± 0.70 ^{b}	14.32 ± 0.53 ^{b}	15.23 ± 1.51 ^{ab}	17.62 ± 1.28 ^{a}
NH_4^+ (mg kg^{-1}) †, §	19.23 ± 0.51 ^{b}	18.38 ± 0.77 ^{b}	19.36 ± 0.56 ^{b}	25.04 ± 0.91 ^{a}	16.85 ± 0.60 ^{b}	12.53 ± 1.25 ^{b}	26.31 ± 1.35 ^{a}	23.00 ± 2.21 ^{a}
NO_3^- (mg kg^{-1}) †, §	0.87 ± 0.12 ^{b}	1.31 ± 0.05 ^{a}	1.09 ± 0.11 ^{ab}	1.04 ± 0.09 ^{b}	0.86 ± 0.08 ^{b}	1.15 ± 0.12 ^{b}	1.44 ± 0.07 ^{a}	1.01 ± 0.06 ^{b}
NO_2^- (μg kg^{-1}) †, §	18.88 ± 1.47 ^{b}	19.99 ± 2.50 ^{b}	23.18 ± 2.37 ^{b}	31.33 ± 1.53 ^{a}	24.51 ± 1.21 ^{b}	27.64 ± 2.52 ^{b}	35.24 ± 1.93 ^{a}	36.51 ± 3.49 ^{a}
Fe(II)/Fe(III) †, §	1.34 ± 0.31 ^{a}	2.18 ± 1.29 ^{a}	0.63 ± 0.03 ^{b}	0.73 ± 0.06 ^{b}	1.97 ± 0.50 ^{a}	1.44 ± 0.11 ^{ab}	1.29 ± 0.49 ^{ab}	1.02 ± 0.03 ^{b}
Sulfide (mg kg^{-1}) †, §	3.48 ± 1.28 ^{b}	2.68 ± 0.19 ^{b}	4.53 ± 1.00 ^{ab}	6.57 ± 0.98 ^{a}	1.25 ± 0.26 ^{b}	2.03 ± 0.48 ^{b}	2.44 ± 0.23 ^{ab}	3.06 ± 0.41 ^{a}
δ^{15}N-NH_4^+ (‰) †, §	8.36 ± 1.33 ^{a}	5.94 ± 0.69 ^{b}	5.91 ± 0.56 ^{b}	5.27 ± 0.35 ^{b}	8.24 ± 2.50 ^{a}	7.26 ± 0.64 ^{a}	7.45 ± 0.83 ^{a}	5.69 ± 0.40 ^{b}
δ^{15}N-NO_3^- (‰)	13.99 ± 1.20 ^{a}	16.59 ± 1.28 ^{a}	15.07 ± 0.65 ^{a}	15.36 ± 0.96 ^{a}	12.33 ± 1.99 ^{a}	15.87 ± 0.15 ^{a}	15.81 ± 2.29 ^{a}	16.56 ± 1.36 ^{a}
δ^{18}O-NO_3^- (‰)	−2.39 ± 0.41 ^{a}	−1.29 ± 0.66 ^{a}	−2.04 ± 0.42 ^{a}	−3.50 ± 1.48 ^{a}	−1.51 ± 0.63 ^{a}	−2.48 ± 0.66 ^{a}	−3.44 ± 0.66 ^{a}	−3.00 ± 1.41 ^{a}

† and § denote that the parameters were significantly different among the saltmarsh stands according to Tukey test at $p < 0.05$, and levels are indicated by different letters

stand compared to native saltmarsh zones, especially in summer, but NO_3^- concentrations did not show a constant trend with plant community stands (Table 1). The Fe(II)/ Fe(III) ratios varied from 0.63 to 2.18 in summer and from 1.02 to 1.97 in winter, and lower ratios were observed in *S. alterniflora* stands (Table 1). Soil δ^{15}N-NH_4^+, δ^{15}N-NO_3^- and δ^{18}O-NO_3^- ranged from 5.27 to 8.36‰, from12.33 to 16.59‰, and from −3.50 to −1.29‰, respectively. *S. alterniflora* stands had slightly lower δ^{15}N-NH_4^+ than other stands, while δ^{15}N-NO_3^- and δ^{18}O-NO_3^- were considerable across the different plant community stands (Table 1).

Significant differences in potential N transformation processes were observed among the saltmarsh zones (Fig. 1). Soil potential nitrification rates in winter were generally higher in *S. alterniflora* stands (0.84 ± 0.02 nmol g^{-1} h^{-1}) than in native saltmarsh zones, while there was no significant difference in summer (Fig. 1). Potential denitrification rates in *S. alterniflora* stands averaged 12.91 ± 0.96 nmol g^{-1} h^{-1} in summer and 1.94 ± 0.23 nmol g^{-1} h^{-1} in winter, and were generally higher than those in bare mudflat and *S. mariqueter* stands (Fig. 1). Potential ANAMMOX rates in *S. alterniflora* stands were significantly higher than those in native saltmarsh zones in summer, but no significant difference was observed among these saltmarsh stands in winter (Fig. 1). Soil potential DNRA rates ranged from 1.12 to 2.11 nmol g^{-1} h^{-1} in summer and from 0.35 to 1.01 nmol g^{-1} h^{-1} in winter. Higher rates were generally observed in *S. alterniflora* stands (Fig. 1).

Potential net N_2O production rates and its isotopic signatures

Potential net N_2O production rates differed by the saltmarsh zones, with values ranging from 0.38 to 0.75 nmol g^{-1} h^{-1} in summer and from 0.13 to 0.16 nmol g^{-1} h^{-1} in winter (Fig. 2). Potential net N_2O production rates in summer were generally lower in *S. alterniflora* stands (0.51 ± 0.07 nmol g^{-1} h^{-1}) than from the bare mudflat (0.75 ± 0.10 nmol g^{-1} h^{-1}) and *S. mariqueter* stands (0.57 ± 0.02 nmol g^{-1} h^{-1}), but slightly higher than those in *P. australis* stands (0.38 ± 0.03 nmol g^{-1} h^{-1}). In contrast, no obvious variations in potential net N_2O production rates among the saltmarsh zones occurred in winter (Fig. 2). The δ^{15}N, δ^{18}O and SP of the emitted N_2O varied from −1.41 to 2.99‰, from 39.66 to 50.38‰, and from 4.09 to 13.69‰, respectively (Fig. S4). δ^{15}N-N_2O correlated positively

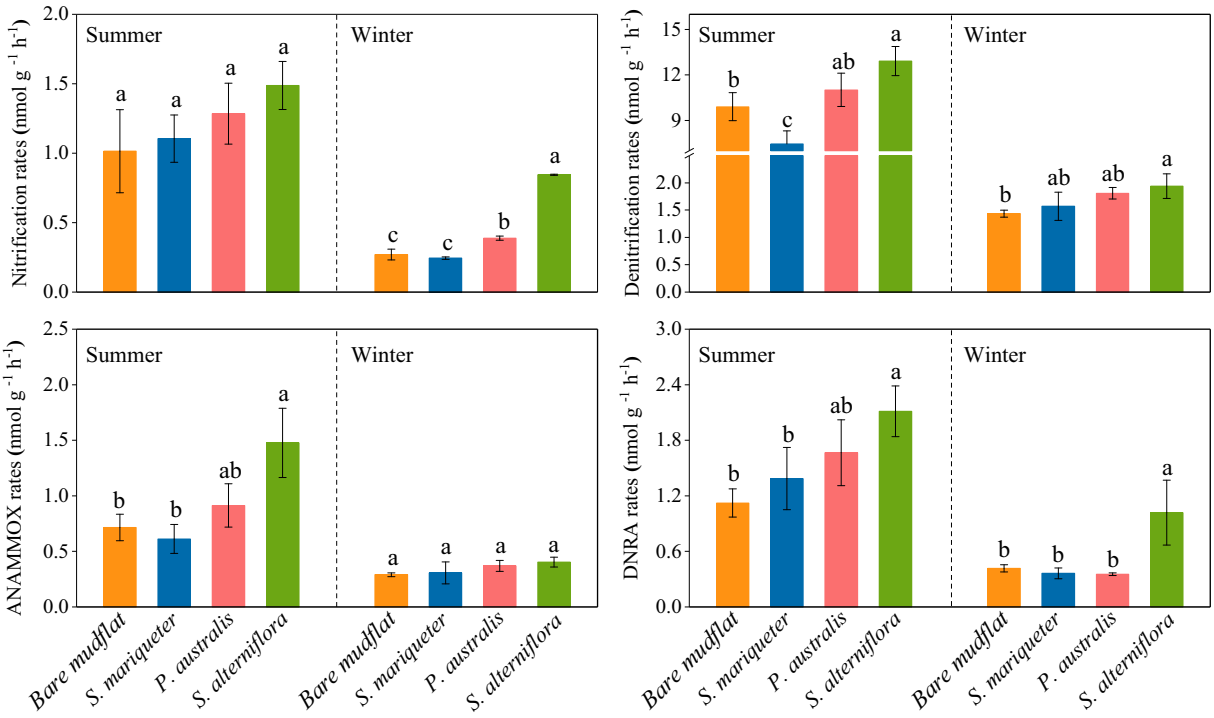

Fig. 1 Potential rates of soil potential nitrification, denitrification, anaerobic ammonium oxidation (ANAMMOX) and dissimilatory nitrate reduction to ammonium (DNRA) rates. Different letters indicate significant differences ($p < 0.05$) at different saltmarsh stands in the same season

with SP-N_2O ($r^2 = 0.44$, $p < 0.01$), while there were no significant correlations of $\delta^{18}O$-N_2O with SP-N_2O and $\delta^{15}N$-N_2O (Fig. S5).

Potential gross N_2O production and consumption rates

Across the saltmarsh zones, potential gross N_2O production and consumption rates varied from 0.68 to 6.06 nmol g^{-1} h^{-1} and from 0.54 to 5.56 nmol g^{-1} h^{-1}, respectively (Fig. 3). *S. alterniflora* and *P. australis* stands had higher potential gross N_2O production and consumption rates, compared to bare mudflat and *S. mariqueter* stands (Fig. 3). Both potential gross production and consumption rates of N_2O were generally higher in summer than in winter (Fig. 3). The proportion of N_2O consumption also differed among the saltmarsh zones, which varied from 68.90 to 92.93% in summer and from 80.38 to 93.16% in winter (Fig. 3). N_2O consumption proportion was significantly higher in *S. alterniflora* and *P. australis* stands than in bare mudflat and *S. mariqueter* stands, especially in summer (Fig. 3).

Soil N_2O source identification

Soil N_2O source changed slightly among the saltmarsh zones (Fig. 4). Of these pathways, denitrification accounted for the highest proportion (69.83 to 80.09%) of soil N_2O source, while NH_2OH oxidation (4.52 to 12.62%) and nitrifier denitrification (13.87 to 21.58%) were also important in N_2O source (Fig. 4).

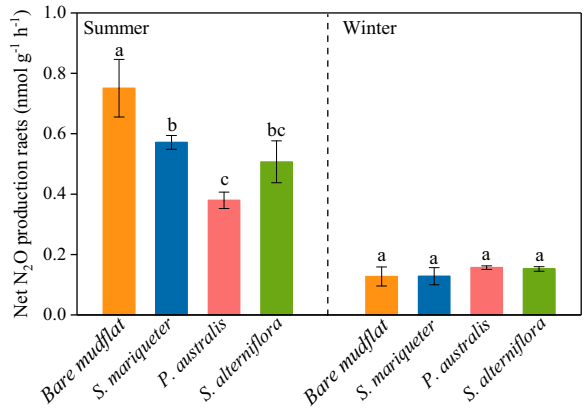

Fig. 2 Soil potential net N_2O production rates. Different letters indicate significant differences ($p < 0.05$) at different saltmarsh stands in the same season

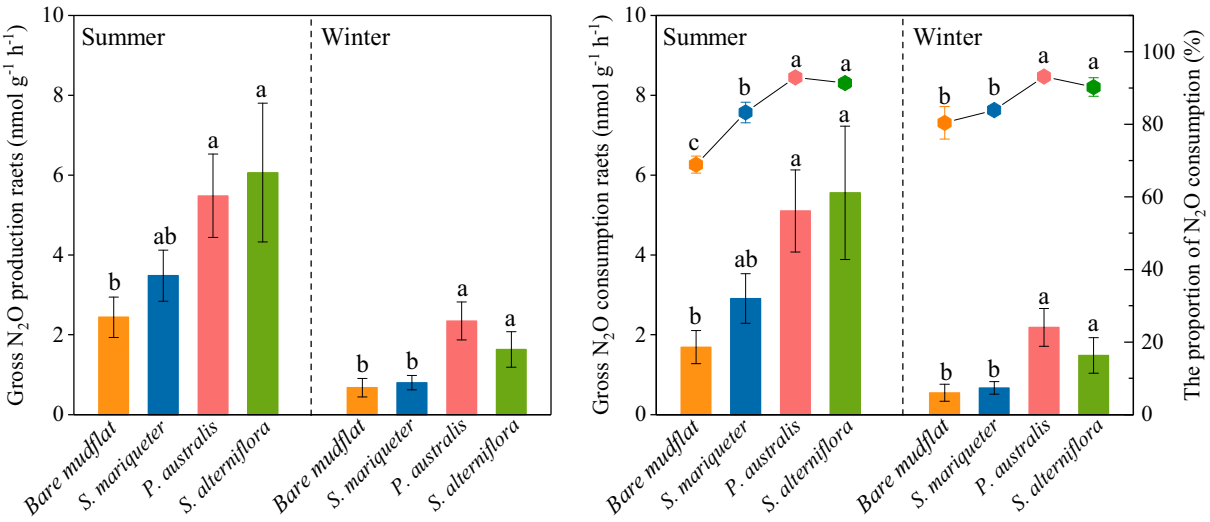

Fig. 3 Soil potential gross N_2O production and consumption rates (bar chart) as well as consumption proportion (scatter chart). Different letters indicate significant differences ($p < 0.05$) at different saltmarsh stands in the same season

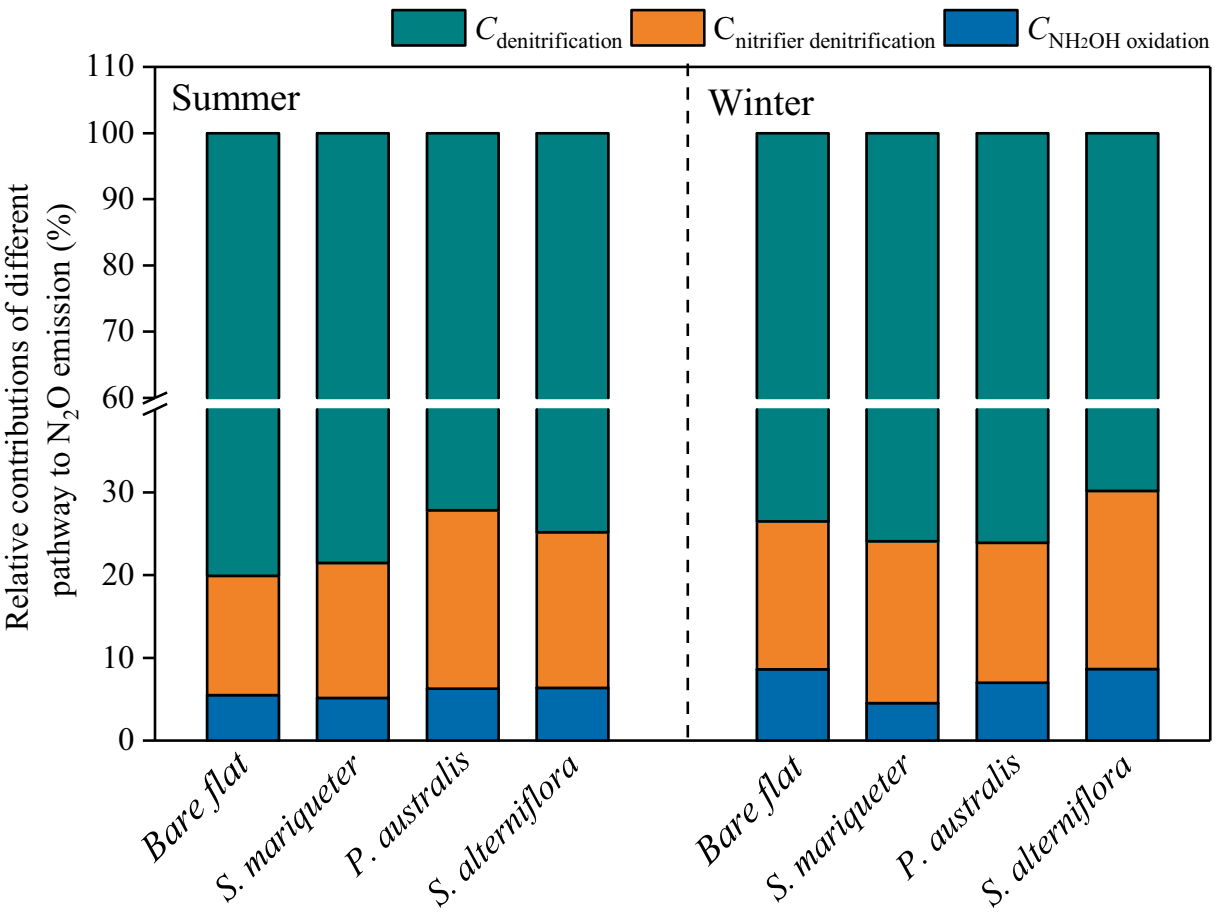

Fig. 4 Relative contributions of NH_2OH oxidation ($C_{NH_2OH\ oxidation}$), denitrification ($C_{denitrification}$) and nitrifier denitrification ($C_{nitrifier\ denitrification}$) to N_2O emission

S. alterniflora stands had higher $C_{\text{nitrifier denitrification}}$ (18.81% for summer and 21.53% for winter) and lower $C_{\text{denitrification}}$ (74.83% for summer and 69.83% for winter) compared to native saltmarsh zones (except *P. australis* stands in summer). With the exception of bare mudflat in winter, $C_{NH_2OH\ \text{oxidation}}$ was generally lower in native saltmarsh zones than in *S. alterniflora* stands (Fig. 4).

Influences of soil variables on potential net N_2O production rates and pathways

Step-wise regression indicated that soil variables explained 39 to 87% of the variations in potential net N_2O production rates and pathways across the saltmarsh zones (Table S2). Summer potential net N_2O production rates were affected by $P_{\text{Gross consumption}}$ ($r^2 = -0.70$, $p < 0.001$), while winter potential net N_2O production was mainly related to salinity, NH_4^+ and bulk density (Table S2). As to N_2O source, $C_{NH_2OH\ \text{oxidation}}$ correlated positively with potential denitrification rates ($r^2 = 0.46$, $p = 0.015$) in summer, but was not related to any of the parameters in winter (Table S2). $C_{\text{nitrifier denitrification}}$ was related to WFPS in summer, but to pH in winter (Table S2). In addition, $C_{\text{denitrification}}$ in summer and winter was negatively correlated with WFPS and DNRA, respectively (Table S2).

Discussion

N_2O emission dynamics

Exotic *S. alterniflora* invasion is an urgent environmental issue, which can regulate estuarine saltmarsh N_2O dynamics by altering biogeochemical processes (Zhang et al. 2013; Yuan et al. 2015; Gao et al. 2019). Across the saltmarsh zones, soil potential net N_2O production rates varied from 0.13 to 0.75 nmol g^{-1} h^{-1}, comparable to the rates reported from other saltmarsh wetlands (Chmura et al. 2011; Moseman-Valtierra et al. 2011; Yang and Silver 2016). Conventionally, soil N_2O production is closely linked to N substrate availability and microbial N-conversation process such as nitrification and/or denitrification (Butterbach-Bahl et al. 2013). In the present study, *S. alterniflora* invasion generally increased carbon and N substrate (NH_4^+ and NO_2^-) concentrations indicating that biomass, root exudate input and decomposition help regulate N substrate concentration (Zhang et al. 2013). In addition, the potential process rates of nitrification and denitrification in *S. alterniflora* stands were often higher than those in bare mudflat and *S. mariqueter* stands, but some differences were not always significant (Fig. 1). These comparisons suggest that *S. alterniflora* stands have higher net N_2O production compared to bare mudflat and *S. mariqueter* stands (Wang et al. 2007). Paradoxically, measured soil potential net N_2O production rates often did not change in this saltmarsh zone (Fig. 2), showing that the drivers of N_2O emission dynamics cannot be discerned by measuring potential net N_2O production and N substrate levels (Yang and Silver 2016). Thus, we further calculated the potential gross N_2O production (0.68 to 6.06 nmol g^{-1} h^{-1}) and consumption rates (0.54 to 5.56 nmol g^{-1} h^{-1}) based on emitted N_2O isotopic ratios. Both were generally higher in *S. alterniflora* and *P. australis* stands than in bare mudflat and *S. mariqueter* (Fig. 3). N_2O consumption in the saltmarsh zones was pronounced, and the higher proportions of N_2O consumption occurred in *S. alterniflora* and *P. australis* stands, especially in summer (Fig. 3). Therefore, we assume that the variations of potential net N_2O production rates in soil following *S. alterniflora* invasion was perhaps caused by the high proportion of N_2O consumption (Jørgensen et al. 2012).

Previous studies indicate that N_2O consumption was related to soil oxygen level, WFPS, substrate availability, sulfide concentration and the DNRA process (Sanford et al. 2012; Yang and Silver 2016). Generally, low soil oxygen availability and reducing conditions favor N_2O consumption via reduction to N_2 (Yang and Silver 2016). Soil aeration condition in *S. alterniflora* and *P. australis* stands may be higher because they have more developed aerenchyma tissue (Yuan et al. 2015) and lower soil WFPF than bare mudflat and *S. mariqueter* stands (Table 1). However, higher biomass and substrate availability are favorable for bacterial activities and soil respiration, which consume oxygen (Metcalfe et al. 2011). These results indicate that soil aeration condition may be unimportant in controlling N_2O consumption in *S. alterniflora* invasion wetland. Sulfide can suppress N_2O reduction to N_2, but *S. alterniflora* is more tolerant to sulfide than native species (Seliskar et al. 2004), which may counteract negative effects. In addition, high sulfide and TOC concentrations can increase the DNRA process, because DNRA uses the electron acceptor (ie., NO_3^-) more efficiently than denitrification in carbon/sulfide-

enriched environments (Kraft et al. 2014). NO_3^- as an electron acceptor can oxidize sulfide to sulfate in sulfide-replete conditions, and the generated sulfate as a competitive electron acceptor may promote DNRA process (Burgin and Hamilton 2008). Meanwhile, DNRA organisms can harbor N_2O reductase encoding gene (i.e., *nosZ*), and accelerate N_2O consumption (Sanford et al. 2012). Indeed, high TOC and sulfide concentrations occurred in *S. alterniflora* and *P. australis* stands, along with greater potential DNRA rates (Table 1 and Fig. 1). These factors contributed to greater N_2O consumption, which may be an important mechanism causing lower or constant potential net N_2O production in *S. alterniflora* stands. Notably, the magnitude of increased N_2O consumption in *S. alterniflora* stands was less pronounced in winter than in summer, likely because the response of N_2O reductase to soil properties variations is less sensitive under low temperature (Holtan-Hartwig et al. 2002). This difference may have led to the seasonal change of *S. alterniflora* invasion influence on potential net N_2O production rates. Kaspar (1982) and Stevens et al. (1998) implied that DNRA can produce N_2O, but the measurement of this process in natural ecosystems is very limited (Murray et al. 2018). Therefore, DNRA does not explain the N_2O production. In short, the complex role of gross N_2O production and consumption processes in regulating N_2O emission at large spatio-temporal scales should be studied further, particularly since invaded *S. alterniflora* may increase the significance of the interaction among carbon, nitrogen and sulfur cycles (Yu et al. 2015).

N_2O source identification based on isotopic signatures

Understanding soil N_2O source is a key to effective mitigation of greenhouse gas in saltmarsh wetlands (Yuan et al. 2015). We attempted to interpret the changes in N_2O source after *S. alterniflora* invasion based on natural isotope analysis. Previous studies found that NH_2OH oxidation and bacteria denitrification (denitrification and nitrifier denitrification) result in higher (33 to 37‰) and lower (−10 to 0‰) SP-N_2O values, respectively (Toyoda et al. 2005; Sutka et al. 2006). Similar to NH_2OH oxidation, SP values of produced N_2O for the fungal denitrification process are often high (Sutka et al. 2008). However, pre-incubation experiments showed that the contribution of fungi to N_2O emission in our study was negligible (Table S1). Moreover, N_2O reduction has a significant effect on isotopic signatures, and the SP-N_2O values increase along with δ^{15}N-N_2O (Ostrom et al. 2007), which is supported by the positive relationships of SP-N_2O and δ^{15}N-N_2O (Fig. S5). Therefore, isotopic analysis based on Monte Carlo method and C_2H_2 inhibition indicated that N_2O emission was driven by denitrification (69.83 to 80.09%), while nitrifier denitrification (13.87 to 21.58%) and NH_2OH oxidation (4.52 to 12.62%) was important to N_2O source (Fig. 4). Estuarine saltmarsh sediment is largely anaerobic, and the substantial contribution of NH_2OH oxidation and nitrifier denitrification to N_2O source in this type of environment might be attributed to the supply of oxygen via plant aerenchyma and tidal action, which is conducive to nitrification (Zhang et al. 2013). Denitrification is the dominant N_2O source in estuarine wetlands (Seitzinger et al. 2000), however the roles of NH_2OH oxidation and nitrifier denitrification in N_2O emission may also be important in these aquatic ecosystems.

Our results revealed that *S. alterniflora* invasion changed N_2O source. $C_{\text{denitrification}}$ in *S. alterniflora* stands generally decreased compared to these native saltmarsh systems (Fig. 4). In denitrification, N_2O is produced as an obligatory intermediate during reduction of NO_3^- to N_2 by heterotrophic denitrifiers (Toyoda et al. 2011). Higher $C_{\text{denitrification}}$ are expected in the stands with higher potential denitrification rates. In our study, the potential DNF rates in *S. alterniflora* stands were generally higher than those in native saltmarsh zones, but not for $C_{\text{denitrification}}$ (Figs. 1 and 4). This result also could be explained by the differences of N_2O consumption during denitrification (Fig. 3). In contrast, $C_{\text{nitrifier denitrification}}$ in *S. alterniflora* stands were slightly increased compared to other saltmarsh stands (except for *P. australis* stands in summer) (Fig. 4). Previous studies indicated that nitrifier denitrification would be favored under fluctuating aerobic-anaerobic environments (Wrage-Mönnig et al. 2018). Among the saltmarsh stands, exotic *S. alterniflora* has considerably higher root systems and lower WFPS, which are conducive to forming this microenvironment (Zhang et al. 2013; Baral et al. 2014). In addition, the change of soil properties driven by plant invasion would influence N_2O source (Wrage-Mönnig et al. 2018). For example, nitrifier denitrification occurred under increasing NO_2^- and decreasing pH conditions (Wrage et al. 2001). In our study, lower soil pH, although not significantly, was observed in *S. alterniflora* stands (Table 1), perhaps due to the greater exudation of organic acids from root

systems (Hines 1994; Bu et al. 2015). Besides, relatively high biomass of *S. alterniflora* can affect root exudates, the source of substrate N, and provide more NO_2^- easily utilized by nitrifier denitrification related microbes (Liao et al. 2008). Stepwise regression analysis also suggests that the variations of $C_{\text{nitrifier denitrification}}$were explained more by soil WFPS and bulk density (Table S2). Notably, $C_{\text{nitrifier denitrification}}$ was also higher at native *P. australis* stands in summer (Fig. 4). To our knowledge, both *P. australis* and *S. alterniflora* have higher biomass and primary productivity, with different seasonal dynamics (Liao et al. 2008). For example, Tong et al. (2011) showed that the belowground biomass in *P. australis* stands was greater than that of *S. alterniflora* in summer, but not in winter. This result could explain why *P. australis* stands exhibited higher $C_{\text{nitrifier denitrification}}$ in summer. Furthermore, it has been noted that N_2O production via NH_2OH oxidation may be triggered by high NH_4^+ and oxygen environments (Wunderlin et al. 2012), which could be responsible for the slight increase in $C_{NH_2OH\ \text{oxidation}}$ in *S. alterniflora* stand compared to native saltmarsh zones (Zhang et al. 2013). However, increased NO_2^- might weaken $C_{NH_2OH\ \text{oxidation}}$, because NH_2OH oxidation is better adapted to low NO_2^- conditions (Wunderlin et al. 2012), which thus complicated NH2OH oxidation contribution in *S. alterniflora* stands. Overall, the effects of plant communities on N_2O emission dynamics are complicated, because they regulate the availability of N substrate and oxygen (Wrage-Mönnig et al. 2018). Our results suggested that if more native saltmarshes are replaced by *S. alterniflora*, the N removal performed by microbial N transformation processes may increase significantly in the Yangtze estuarine wetlands, but it may be not the case for N_2O emission.

Conclusions

This study reports soil potential N_2O production and consumption processes following exotic *S. alterniflora* invasion in estuarine saltmarsh wetlands. *S. alterniflora* invasion slightly decreased soil potential net N_2O production rates. The variations in gross N_2O consumption proportion drove potential net N_2O production across the saltmarsh wetlands. In addition to denitrification, NH_2OH oxidation and nitrifier denitrification were also important in N_2O production. *S. alterniflora* invasion enhanced the contribution of NH_2OH oxidation and nitrifier denitrification to the production of N_2O, but decreased the contribution of denitrification. The variations of soil WPFS, pH, sulfide and substrate availability caused by plant invasion were the underlying factors influencing N_2O dynamics. Overall, this study provides a valuable perspective on the mechanisms controlling N_2O production and consumption processes in estuarine saltmarsh wetlands.

Acknowledgments This work was funded by the Natural Science Foundation of China (Nos. 41671463, 41725002, 41761144062, 41730646, and 41601530). It was also supported by Chinese National Key Programs for Fundamental Research and Development (Nos. 2016YFA0600904, and 2016YFE0133700), Fundamental Research Funds for the Central Universities, and the Yangtze Delta Estuarine Wetland Station (ECNU). We thank Wayne S. Gardner, anonymous reviewers and editor for constructive comments and valuable suggestions on this manuscript.

References

Allen DE, Dalal RC, Rennenberg H, Meyer RL, Reeves S, Schmidt S (2007) Spatial and temporal variation of nitrous oxide and methane flux between subtropical mangrove sediments and the atmosphere. Soil Biol Biochem 39:622–631

Baral BR, Kuyper TW, Van Groenigen JW (2014) Liebig's law of the minimum applied to a greenhouse gas: alleviation of P-limitation reduces soil N_2O emission. Plant Soil 374:539–548

Bowden WB (1986) Nitrification, nitrate reduction, and nitrogen immobilization in a tidal freshwater marsh sediment. Ecology 67:88–99

Bu N, Qu JF, Li ZL, Li G, Zhao H, Zhao B, Chen JK, Fang CM (2015) Effects of *Spartina alterniflora* invasion on soil respiration in the Yangtze River estuary, China. PLoS One 10: e0121571

Butterbach-Bahl K, Baggs EM, Dannenmann M, Kiese R, Zechmeister-Boltenstern S (2013) Nitrous oxide emissions from soils: how well do we understand the processes and their controls? Philos T R Soc B 368:20130122

Burgin AJ, Hamilton SK (2008) NO_3^--driven SO_4^{2-} production in freshwater ecosystems: implications for N and S cycling. Ecosystems 11:908–922

Canfield DE, Glazer AN, Falkowski PG (2010) The evolution and future of Earth's nitrogen cycle. Science 330:192–196

Cheng XL, Peng RH, Chen JQ, Luo YQ, Zhang QF, An SQ, Chen JK, Li B (2007) CH_4 and N_2O emissions from *Spartina alterniflora* and *Phragmites australis* in experimental mesocosms. Chemosphere 68:420–427

Chmura GL, Kellman L, Guntenspergen GR (2011) The greenhouse gas flux and potential global warming feedbacks of a northern macrotidal and microtidal salt marsh. Environ Res Lett 6:044016

Cline JD (1969) Spectrophotometric determination of hydrogen sulfide in natural waters. Limnol Oceanogr 14:454–458

Cohen Y, Gordon LI (1978) Nitrous oxide in the oxygen minimum of the eastern tropical North Pacific: evidence for its consumption during denitrification and possible mechanisms for its production. Deep-Sea Res 25:509–524

Deng F, Hou L, Liu M, Zheng Y, Yin G, Li X, Jiang X (2015) Dissimilatory nitrate reduction processes and associated contribution to nitrogen removal in sediments of the Yangtze estuary. J Geophys Res Biogeosci 120:1521–1531

Deppe M, Well R, Giesemann A, Spott O, Flessa H (2017) Soil N_2O fluxes and related processes in laboratory incubations simulating ammonium fertilizer depots. Soil Biol Biochem 104:68–80

Dollhopf SL, Hyun JH, Smith AC, Adams HJ, O'Brien S, Kostka JE (2005) Quantification of ammonia-oxidizing bacteria and factors controlling nitrification in salt marsh sediments. Appl Environ Microbiol 71:240–246

Dong LF, Nedwell DB, Underwood GJ, Thornton DC, Rusmana I (2002) Nitrous oxide formation in the Colne estuary, England: the central role of nitrite. Appl Environ Micro 68: 1240–1249

Firestone MK, Davidson EA (1989) Microbiological basis of NO and N_2O production and consumption in soil. Exchange of trace gases between terrestrial ecosystems and the atmosphere: report of the Dahlem workshop on exchange of trace gases between terrestrial ecosystems and the atmosphere, Berlin 1989, February 19–24. Wiley, pp 7–21

Gao D, Li X, Lin X, Wu D, Jin B, Huang Y, Liu M, Chen X (2017) Soil dissimilatory nitrate reduction processes in the *Spartina alterniflora* invasion chronosequences of a coastal wetland of southeastern China: dynamics and environmental implications. Plant Soil 421:383–399

Gao GF, Li PF, Zhong JX, Shen ZJ, Chen J, Li YT, Isabwe A, Zhu XY, Ding QS, Zhang S, Gao CH, Zheng HL (2019) *Spartina alterniflora* invasion alters soil bacterial communities and enhances soil N_2O emissions by stimulating soil denitrification in mangrove wetland. Sci Total Environ 653:231–240

Hines ME (1994) Acetate concentrations and oxidation in salt-marsh sediments. Limnol Oceanogr 39:140–148

Holtan-Hartwig L, Dörsch P, Bakken LR (2002) Low temperature control of soil denitrifying communities: kinetics of N_2O production and reduction. Soil Biol Biochem 34:1797–1806

Hou L, Zheng Y, Liu M, Gong J, Zhang XL, Yin GY, You L (2013) Anaerobic ammonium oxidation (anammox) bacterial diversity, abundance, and activity in marsh sediments of the Yangtze estuary. J Geophys Res Biogeosci 118:1237–1246

Ishii S, Song Y, Rathnayake L, Tumendelger A, Satoh H, Toyoda S, Okabe S (2014) Identification of key nitrous oxide production pathways in aerobic partial nitrifying granules. Environ Microbiol 16:3168–3180

Jia D, Qi F, Xu X, Feng J, Wu H, Guo J, Lin G (2016) Co-regulations of *Spartina alterniflora* invasion and exogenous nitrogen loading on soil N_2O efflux in subtropical mangrove mesocosms. PLoS One 11:e0146199

Jørgensen CJ, Struwe S, Elberling B (2012) Temporal trends in N_2O flux dynamics in a Danish wetland–effects of plant-mediated gas transport of N_2O and O_2 following changes in water level and soil mineral-N availability. Glob Chang Biol 18:210–222

Kaspar HF (1982) Nitrite reduction to nitrous oxide by propionibacteria: detoxication mechanism. Arch Microbiol 133:126–130

Koba K, Osaka K, Tobari Y, Toyoda S, Ohte N, Katsuyama M, Suzuki N, Itoh M, Yamagishi H, Kawasaki M, Kim SJ, Yoshida N, Nakajima T (2009) Biogeochemistry of nitrous oxide in groundwater in a forested ecosystem elucidated by nitrous oxide isotopomer measurements. Geochim Cosmochim Ac 73:3115–3133

Kraft B, Tegetmeyer HE, Sharma R, Klotz MG, Ferdelman TG, Hettich RL, Strous M (2014) The environmental controls that govern the end product of bacterial nitrate respiration. Science 345:676–679

Li B, Liao CH, Zhang XD, Chen HL, Wang Q, Chen ZY, Cheng XL (2009) *Spartina alterniflora* invasions in the Yangtze River estuary, China: an overview of current status and ecosystem effects. Ecol Eng 35:511–520

Liao CZ, Luo YQ, Fang CM, Chen JK, Li B (2008) Litter pool sizes, decomposition, and nitrogen dynamics in *Spartina alterniflora*-invaded and native coastal marshlands of the Yangtze estuary. Oecologia 156:589–600

Lovley DR, Phillips EJ (1987) Rapid assay for microbially reducible ferric iron in aquatic sediments. Appl Environ Microb 53:1536–1540

Lu J, Zhang Y (2013) Spatial distribution of an invasive plant *Spartina alterniflora* and its potential as biofuels in China. Ecol Eng 52:175–181

Lu R (2000) Methods of soil and agro-chemical analysis. China Agric Sci Tech Press, Beijing

Metcalfe DB, Fisher RA, Wardle DA (2011) Plant communities as drivers of soil respiration: pathways, mechanisms, and significance for global change. Biogeosciences 8:2047–2061

Murray R, Erler D, Rosentreter J, Maher D, Eyre B (2018) A seasonal source and sink of nitrous oxide in mangroves: insights from concentration, isotope, and isotopomer measurements. Geochim Cosmochim Ac 238:169–192

Moseman-Valtierra S, Gonzalez R, Kroeger KD, Tang J, Chao WC, Crusius J, Shelton J (2011) Short-term nitrogen additions can shift a coastal wetland from a sink to a source of N_2O. Atmos Environ 45:4390–4397

Onley JR, Ahsan S, Sanford RA, Löffler FE (2018) Denitrification by Anaeromyxobacter dehalogenans, a common soil bacterium lacking the nitrite reductase genes *nirS* and *nirK*. Appl Environ Microb 84:e01985–e01917

Ostrom NE, Pitt A, Sutka R, Ostrom PH, Grandy AS, Huizinga KM, Robertson GP (2007) Isotopologue effects during N_2O reduction in soils and in pure cultures of denitrifiers. J Geophys Res Biogeosci 112:G02005

Peng RH, Fang CM, Li B, Chen JK (2011) *Spartina alterniflora* invasion increases soil inorganic nitrogen pools through interactions with tidal subsidies in the Yangtze estuary, China. Oecologia 165:797–807

Ravishankara AR, Daniel JS, Portmann RW (2009) Nitrous oxide (N_2O): the dominant ozone-depleting substance emitted in the 21st century. Science 326:123–125

Robertson GP (1987) Nitrous oxide sources in aerobic soils: nitrification, denitrification and other biological processes. Soil Biol Biochem 19:187–193

Sanford RA, Wagner DD, Wu Q, Chee-Sanford JC, Thomas SH, Cruz-García C, Nissen S (2012) Unexpected nondenitrifier nitrous oxide reductase gene diversity and abundance in soils. P Natl Acad Sci USA 109:19709–19714

Seitzinger SP, Kroeze C, Styles RV (2000) Global distribution of N_2O emissions from aquatic systems: natural emissions and anthropogenic effects. Chemosphere Global Change Sci 2: 267–279

Seliskar DM, Smart KE, Higashikubo BT, Gallagher JL (2004) Seedling sulfide sensitivity among plant species colonizing Phragmites-infested wetlands. Wetlands 24:426–433

Shoun H, Tanimoto T (1991) Denitrification by the fungus Fusarium oxysporum and involvement of cytochrome P-450 in the respiratory nitrite reduction. J Biol Chem 266: 11078–11082

Sørensen J, Tiedje JM, Firestone RB (1980) Inhibition by sulfide of nitric and nitrous oxide reduction by denitrifying *Pseudomonas fluorescens*. Appl Environ Microbiol 39: 105–108

Stribling JM, Cornwell JC (2001) Nitrogen, phosphorus, and sulfur dynamics in a low salinity marsh system dominated by *Spartina alterniflora*. Wetlands 21:629–638

Sun Z, Sun W, Tong C, Zeng C, Yu X, Mou X (2015) China's coastal wetlands: conservation history, implementation efforts, existing issues and strategies for future improvement. Environ Int 79:25–41

Sutka RL, Ostrom NE, Ostrom PH, Gandhi H, Breznak JA (2003) Nitrogen isotopomer site preference of N_2O produced by *Nitrosomonas europaea* and *Methylococcus capsulatus* Bath. Rapid Commun Mass Sp 17:738–745

Sutka RL, Ostrom NE, Ostrom PH, Breznak JA, Gandhi H, Pitt AJ, Li F (2006) Distinguishing nitrous oxide production from nitrification and denitrification on the basis of isotopomer abundances. Appl Environ Microb 72:638–644

Sutka RL, Adams GC, Ostrom NE, Ostrom PH (2008) Isotopologue fractionation during N_2O production by fungal denitrification. Rapid Commun Mass Sp 22:3989–3996

Stevens RJ, Laughlin RJ, Malone JP (1998) Soil pH affects the processes reducing nitrate to nitrous oxide and di-nitrogen. Soil Biol Biochem 30:1119–1126

Tiedje JM, Sexstone AJ, Myrold DD, Robinson JA (1983) Denitrification: ecological niches, competition and survival. Anton Leeuw Int J G 48:569–583

Thamdrup B, Dalsgaard T (2002) Production of N_2 through anaerobic ammonium oxidation coupled to nitrate reduction in marine sediments. Appl Environ Microb 68:1312–1318

Tong C, Zhang L, Wang W, Gauci V, Marrs R, Liu B, Zeng C (2011) Contrasting nutrient stocks and litter decomposition in stands of native and invasive species in a sub-tropical estuarine marsh. Environ Res 111:909–916

Toyoda S, Yano M, Nishimura SI, Akiyama H, Hayakawa A, Koba K, Ogawa NO (2011) Characterization and production and consumption processes of N_2O emitted from temperate agricultural soils determined via isotopomer ratio analysis. Global Biogeochem Cy 25:96–101

Toyoda S, Mutobe H, Yamagishi H, Yoshida N, Tanji Y (2005) Fractionation of N_2O isotopomers during production by denitrifier. Soil Biol Biochem 37:1535–1545

Wang DQ, Chen ZL, Wang J, Xu SY, Yang HX, Chen H, Yang LY, Hu LZ (2007) Summer-time denitrification and nitrous oxide exchange in the intertidal zone of the Yangtze estuary. Estuar Coast Shelf S 73:43–53

Wei J, Zhou M, Vereecken H, Brüggemann N (2017) Large variability in CO_2 and N_2O emissions and in ^{15}N site preference of N_2O from reactions of nitrite with lignin and its derivatives at different pH. Rapid Commun Mass Sp 31: 1333–1343

Wrage N, Velthof GL, Van Beusichem ML, Oenema O (2001) Role of nitrifier denitrification in the production of nitrous oxide. Soil Biol Biochem 33:1723–1732

Wrage-Mönnig N, Horn MA, Well R, Müller C, Velthof G, Oenema O (2018) The role of nitrifier denitrification in the production of nitrous oxide revisited. Soil Biol Biochem 123: A3–A16

Wu LB, Liu XD, Fang YT, Hou SJ, Xu LQ, Wang XY, Fu PQ (2018) Nitrogen cycling in the soil–plant system along a series of coral islands affected by seabirds in the South China Sea. Sci Total Environ 627:166–175

Wunderlin P, Mohn J, Joss A, Emmenegger L, Siegrist H (2012) Mechanisms of N_2O production in biological wastewater treatment under nitrifying and denitrifying conditions. Water Res 46:1027–1037

Wunderlin P, Lehmann MF, Siegrist H, Tuzson B, Joss A, Emmenegger L, Mohn J (2013) Isotope signatures of N_2O in a mixed microbial population system: constraints on N_2O producing pathways in wastewater treatment. Environ Sci Technol 47:1339–1348

Yang W, Yan YE, Jiang F, Leng X, Chen XL, An SQ (2016) Response of the soil microbial community composition and biomass to a short-term *Spartina alterniflora* invasion in a coastal wetland of eastern China. Plant Soil 408:443–456

Yang WH, Teh YA, Silver WL (2011) A test of a field-based 15 N–nitrous oxide pool dilution technique to measure gross N_2O production in soil. Glob Chang Biol 17:3577–3588

Yang WH, Silver WL (2016) Gross nitrous oxide production drives net nitrous oxide fluxes across a salt marsh landscape. Glob Chang Biol 22:2228–2237

Yin GY, Hou LJ, Liu M, Liu ZF, Gardner WS (2014) A novel membrane inlet mass spectrometer method to measure $15NH_4^+$ for isotope-enrichment experiments in aquatic ecosystems. Environ Sci Technol 48:9555–9562

Yin GY, Hou LJ, Liu M, Li XF, Zheng YL, Gao J, Lin XB (2017) DNRA in intertidal sediments of the Yangtze estuary. J Geophys Res Biogeosci 122:1988–1998

Yu X, Yang J, Liu L, Tian Y, Yu Z (2015) Effects of *Spartina alterniflora* invasion on biogenic elements in a subtropical coastal mangrove wetland. Environ Sci Pollut R 22:3107–3115

Yuan J, Ding W, Liu D, Kang H, Freeman C, Xiang J, Lin Y (2015) Exotic *Spartina alterniflora* invasion alters ecosystem–atmosphere exchange of CH_4 and N_2O and carbon sequestration in a coastal salt marsh in China. Glob Chang Biol 21:1567–1580

Zhang WL, Zeng CS, Tong C, Zhai SJ, Lin X, Gao DZ (2015) Spatial distribution of phosphorus speciation in marsh sediments along a hydrologic gradient in a subtropical estuarine wetland, China. Estuar Coast Shelf S 154:30–38

Zhang Y, Wang L, Xie X, Huang L, Wu Y (2013) Effects of invasion of *Spartina alterniflora* and exogenous N deposition on N_2O emissions in a coastal salt marsh. Ecol Eng 58: 77–83

Zhang W, Li Y, Xu C, Li Q, Lin W (2016) Isotope signatures of N_2O emitted from vegetable soil: Ammonia oxidation drives N_2O production in NH_4^+-fertilized soil of North China. Sci Rep 6:29257

Zheng YL, Hou LJ, Liu M, Yin GY, Gao J, Jiang XF, Wang R (2016) Community composition and activity of anaerobic ammonium oxidation bacteria in the rhizosphere of salt-marsh grass *Spartina alterniflora*. Appl Microbiol Biot 100: 8203–8212

Zhu X, Burger M, Doane TA, Horwath WR (2013) Ammonia oxidation pathways and nitrifier denitrification are significant sources of N_2O and NO under low oxygen availability. P Natl Acad Sci USA 110:201219993

Zou Y, Hirono Y, Yanai Y, Hattori S, Toyoda S, Yoshida N (2014) Isotopomer analysis of nitrous oxide accumulated in soil cultivated with tea (*Camellia sinensis*) in Shizuoka, Central Japan. Soil Biol Biochem 77:276–291